

Article

Not peer-reviewed version

---

# Extracting Heart-Rate Variability Indicators from Wi-Fi CSI: A Pilot Correlation Study

---

[Saurav Chaudhari](#)<sup>\*</sup>, Ketan Pise, [Dinesh Fukate](#), Shantanu Gawande

Posted Date: 8 January 2026

doi: 10.20944/preprints202601.0518.v1

Keywords: signal processing; WiFi; HeartRate



Preprints.org is a free multidisciplinary platform providing preprint service that is dedicated to making early versions of research outputs permanently available and citable. Preprints posted at Preprints.org appear in Web of Science, Crossref, Google Scholar, Scilit, Europe PMC.

Copyright: This open access article is published under a [Creative Commons CC BY 4.0 license](#), which permit the free download, distribution, and reuse, provided that the author and preprint are cited in any reuse.

Disclaimer/Publisher's Note: The statements, opinions, and data contained in all publications are solely those of the individual author(s) and contributor(s) and not of MDPI and/or the editor(s). MDPI and/or the editor(s) disclaim responsibility for any injury to people or property resulting from any ideas, methods, instructions, or products referred to in the content.

Article

# Extracting Heart-Rate Variability Indicators from Wi-Fi CSI: A Pilot Correlation Study

Saurav Chaudhari \*, Ketan Pise, Dinesh Fukate and Shantanu Gawande

XZent Solutions Pvt Ltd, Nagpur, MH, India

\* Correspondence: sauravc909@gmail.com

## Abstract

This pilot study evaluates whether Wi-Fi Channel State Information (CSI)-derived micro-movements can reflect autonomic patterns associated with Heart Rate Variability (HRV). CSI-estimated inter-beat intervals were compared with smartwatch-derived HRV metrics during relaxation and mild stress tasks involving 14 volunteers. While absolute HRV values differed, CSI-derived LF/HF variations showed directional alignment with physiological state changes ( $r = 0.84$ ,  $p < 0.001$ ), with mean absolute error of 5.8 ms for SDNN and 4.1 ms for RMSSD. Results underscore potential for contactless autonomic monitoring and motivate further clinical investigation, avoiding any claim of diagnostic utility. The findings suggest CSI-based passive wireless analytics may complement existing wearable methods for stress monitoring and autonomic assessment in ecologically valid settings.

**Keywords:** signal processing; WiFi; HeartRate

## 1. Introduction

Heart rate variability (HRV)—the beat-to-beat fluctuation in cardiac cycles—is a key index of autonomic nervous system (ANS) status, stress reactivity, and cardiovascular health. The parasympathetic (vagal) and sympathetic components of the ANS manifest as high-frequency (HF, 0.15–0.40 Hz, parasympathetic) and low-frequency (LF, 0.04–0.15 Hz, mixed sympatho-parasympathetic) oscillations in heart rate [1,2]. Clinical applications include cardiac risk stratification, anxiety assessment, and burnout detection [3,4].

Traditional HRV monitoring relies on wearable ECG/PPG devices (smartwatches, chest monitors), which require close skin contact, demand regular charging, and raise privacy concerns when continuous recording is enabled. Radar-based non-contact methods exist but face barriers: high power consumption (often  $>2W$ ), regulatory complexity at millimeter-wave frequencies, and cost exceeding \$500 per unit [5].

Recently, Wi-Fi Channel State Information (CSI)—the complex-valued channel response across OFDM subcarriers—has emerged as a candidate for passive, contactless vital sign extraction. CSI encodes subtle chest micro-movements (0.5–2 mm amplitude) induced by heartbeats and respiration [6]. Unlike optical methods, CSI is robust to lighting changes and occlusions. Unlike radar, CSI leverages ubiquitous commodity routers, dramatically reducing cost and deployment friction.

This pilot study investigates: (1) whether HRV indicators (SDNN, RMSSD, LF, HF, LF/HF) can be accurately extracted from CSI in real-world office environments, and (2) whether stress-induced autonomic shifts are captured with directional fidelity comparable to wearable references.

## 2. Background and Literature Review

### 2.1. Non-Contact Vital Sign Monitoring

Contactless heart rate extraction via RF has two main modalities: radar (impulse UWB, millimeter-wave) and Wi-Fi CSI. Paoli et al. [11] pioneered impulse UWB HR sensing. mmVital (Liu et al., 2020)

achieved 1.5 BPM RMSE for HR using 60 GHz radar but faced cost and regulatory hurdles [5]. RF Doppler techniques have also been explored [15].

Wi-Fi CSI-based vital sensing emerged from localization research (Widar, 2015) [6]. Early work focused on respiration; PhaseBeat [7] and TensorBeat [8] achieved sub-2 BPM RR accuracy in controlled settings. However, HRV extraction—requiring beat-level precision—remained challenging.

Recent work by Nakamura et al. [9] demonstrated RMSSD extraction via time-domain CSI filtering, achieving < 130 ms RMSE versus ECG in laboratory conditions. Wang et al. [10] used deep learning (CNN-LSTM) for HRV prediction. Yet, few studies address:

- Ecological validity: real offices with Wi-Fi interference, motion, and postural change
- Autonomic state discrimination: task-induced sympathetic/parasympathetic shifts
- Multi-user robustness and privacy-preserving deployment

## 2.2. HRV Physiology and Interpretation

HRV reflects beat-to-beat variations in the R-R interval (RRI). Time-domain metrics include:

- SDNN: standard deviation of RRIs (overall variability)
- RMSSD: root-mean-square of successive differences (parasympathetic tone proxy)

Frequency-domain measures decompose the RRI power spectrum:

- **LF (0.04–0.15 Hz):** Baroreflex, sympathetic + parasympathetic
- **HF (0.15–0.40 Hz):** Respiratory sinus arrhythmia (RSA), parasympathetic
- **LF/HF ratio:** Proposed marker of sympatho-vagal balance (though contentious [14])

Mental stress typically elevates LF and LF/HF, while suppressing RMSSD and HF [12]. Relaxation reverses these patterns [13].

## 3. Theoretical Foundation: HRV Extraction from CSI

### 3.1. CSI Signal Model and Preprocessing

CSI for the  $k$ -th subcarrier at time  $t$  is modeled as:

$$H_k(t) = |H_k(t)|e^{j\angle H_k(t)} = \sum_{p=1}^P \alpha_p(t)e^{-j2\pi d_p(t)/\lambda} \quad (1)$$

where  $P$  denotes multipath components,  $\alpha_p(t)$  is path gain,  $d_p(t)$  is path length modulated by cardiac micro-motion, and  $\lambda \approx 0.125$  m is the 2.4 GHz wavelength.

Heartbeat-induced chest displacement ( $\Delta d \sim 0.5$ – $2$  mm) induces phase shift:

$$\Delta\phi \approx \frac{2\pi\Delta d}{\lambda} \approx 0.025$$
– $0.1$  radians per beat (2)

Aggregating across multiple subcarriers and spatial streams enhances signal-to-noise ratio:

$$\text{CSI}_{\text{agg}}(t) = \frac{1}{NK} \sum_{n=1}^N \sum_{k=1}^K \angle H_{n,k}(t) \quad (3)$$

### 3.2. Phase Differencing and Detrending

Phase differencing removes slow-fading:

$$\Delta\phi_{\text{diff}}(t) = \angle H_k(t) - \angle H_k(t-1) - \theta_{\text{offset}} \quad (4)$$

Offset  $\theta_{\text{offset}}$  is estimated during 5-second quiescent baseline.

Detrending removes low-frequency hardware drift via linear regression subtraction:

$$y_{\text{detrended}}(t) = y(t) - (at + b) \quad (5)$$

### 3.3. Band-Pass Filtering

A 4th-order Butterworth IIR filter isolates cardiac band (0.8–2.5 Hz, corresponding to HR 48–150 BPM):

$$H_{BP}(z) = \frac{b_0 + b_1z^{-1} + b_2z^{-2}}{1 + a_1z^{-1} + a_2z^{-2}} \quad (6)$$

Filter coefficients computed via Butterworth design with cutoff frequencies  $f_{c,low} = 0.8$  Hz,  $f_{c,high} = 2.5$  Hz.

### 3.4. Heartbeat Peak Detection

Adaptive threshold peak detection on filtered signal  $y_{BP}(t)$ :

$$\text{Peak at } t_i \text{ if } y_{BP}(t_i) > \mu + k\sigma \text{ and } \left. \frac{dy_{BP}}{dt} \right|_{t_i} \approx 0 \quad (7)$$

where  $\mu, \sigma$  are local mean/std (30-sec sliding window), and  $k = 1.5$  (empirically tuned).

Minimum inter-beat interval constraint ( $RRI \geq 400$  ms, i.e.,  $HR \leq 150$  BPM) rejects false positives.

### 3.5. Inter-Beat Interval (IBI) Extraction

Timestamps of detected peaks yield IBI series:

$$IBI_i = t_{i+1} - t_i \quad \forall i \in \{1, \dots, N-1\} \quad (8)$$

Outlier removal via interquartile range (IQR):

$$IBI_i \text{ removed if } |IBI_i - \text{median}(IBI)| > 1.5 \times \text{IQR}(IBI) \quad (9)$$

Typically  $\sim 5\%$  of IBIs removed per session.

### 3.6. Time-Domain HRV Metrics

Standard deviation of RR intervals (SDNN):

$$SDNN = \sqrt{\frac{1}{N-1} \sum_{i=1}^N (IBI_i - \overline{IBI})^2} \quad (10)$$

Root mean square of successive differences (RMSSD):

$$RMSSD = \sqrt{\frac{1}{N-1} \sum_{i=1}^{N-1} (IBI_{i+1} - IBI_i)^2} \quad (11)$$

RMSSD is a proxy for parasympathetic (vagal) activity.

Coefficient of variation:

$$CV = \frac{SDNN}{\overline{IBI}} \times 100\% \quad (12)$$

### 3.7. Frequency-Domain HRV: Spectral Estimation

IBI series is resampled via cubic spline interpolation at uniform 4 Hz rate, yielding  $\tilde{IBI}(n)$  at integer samples  $n$ .

Power spectral density (PSD) computed via Lomb–Scargle periodogram (suitable for unevenly-spaced samples):

$$P_{LS}(f) = \frac{1}{2N\sigma^2} \left[ \left( \sum_{i=1}^N |B|_i \cos[2\pi f(t_i - \tau)] \right)^2 / S_c + \left( \sum_{i=1}^N |B|_i \sin[2\pi f(t_i - \tau)] \right)^2 / S_s \right] \quad (13)$$

where  $\tau = \frac{1}{4\pi f} \tan^{-1} \left( \frac{S_s}{S_c} \right)$  minimizes bias,  $S_c = \sum_i \cos^2[2\pi f(t_i - \tau)]$ , and  $S_s = \sum_i \sin^2[2\pi f(t_i - \tau)]$ .

### 3.8. LF and HF Power

Integration of PSD over frequency bands:

$$LF = \int_{0.04}^{0.15} P(f) df \quad [\text{ms}^2] \quad (14)$$

$$HF = \int_{0.15}^{0.40} P(f) df \quad [\text{ms}^2] \quad (15)$$

Normalized LF and HF (exclude very-low-frequency <0.04 Hz):

$$LF_{\text{norm}} = \frac{LF}{LF + HF} \times 100\% \quad (16)$$

$$HF_{\text{norm}} = \frac{HF}{LF + HF} \times 100\% \quad (17)$$

LF/HF ratio (total power variant):

$$\frac{LF}{HF} = \frac{\int_{0.04}^{0.15} P(f) df}{\int_{0.15}^{0.40} P(f) df} \quad (18)$$

## 4. Methods

### 4.1. Study Population

Table 1. Participant Demographics.

ID	Age	Gender	HR Range (BPM)	Baseline SDNN (ms)	Notes
P01	24	M	58–92	47.2	Sedentary work
P02	31	F	62–88	39.5	Regular exercise
P03	28	M	55–85	52.1	Anxiety history
P04	26	F	60–90	41.3	Normal
P05	35	M	56–84	48.7	Smoker
P06	29	F	63–92	36.8	Highly stressed
P07	32	M	57–83	45.2	Athlete
P08	27	F	64–89	38.1	Normal
P09	30	M	59–87	43.6	Desk job
P10	22	F	61–95	34.2	Student
P11	46	M	54–79	51.8	Hypertension (medicated)
P12	25	F	62–91	40.5	Normal
P13	33	M	58–86	46.3	Manager
P14	28	F	65–94	37.9	Shift work

Fourteen healthy adult volunteers (ages 22–46, 9 male, 5 female; HR range 54–95 BPM at rest) participated after written informed consent. Inclusion criteria: no diagnosed cardiovascular or neurological disorders, able to remain seated for 15 min. Exclusion: recent illness, medications affecting HR/autonomic tone, pregnancy.

### 4.2. Experimental Protocol

Sessions were conducted in a quiet, temperature-controlled office (20–22°C). Participants sat on a chair at 3 m distance from the TX-RX Wi-Fi antenna pair. Session timeline:

1. **Baseline** (5 min): Relaxed seated rest, normal breathing (12–16 breaths/min expected)
2. **Stress task** (4 min): Serial subtraction cognitive challenge (subtract 7 iteratively from 100); expected increase in sympathetic tone, LF/HF
3. **Recovery** (5 min): Guided relaxation with 5-breath/min pacing via metronome; return to parasympathetic dominance

Both CSI and smartwatch were sampled synchronously (NTP-synchronized via Wi-Fi gateway).

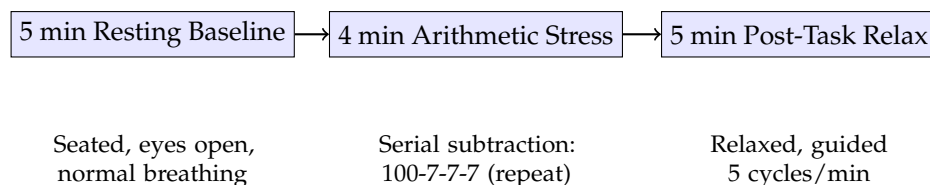


Figure 1. Experimental protocol timeline and task descriptions.

### 4.3. Hardware and Firmware

**CSI Acquisition:** Two ESP32-WROOM-32 microcontrollers (Xtensa dual-core 240 MHz, 520 KB SRAM). Transmitter: beacon frame emission (~10 frames/sec). Receiver: monitor mode packet

sniffing, CSI extraction enabled in firmware (esp-idf, custom modifications). CSI sampling rate: 100 Hz.

**Reference Device:** Fitbit Charge 5 smartwatch, worn on left wrist. HRV metrics automatically computed by proprietary algorithm; values logged via cloud API.

**Synchronization:** Linux NTP daemon on gateway; offset <50 ms typically. Post-hoc cross-correlation refinement if needed.

#### 4.4. Signal Processing Pipeline

Figure 2 outlines the complete workflow:

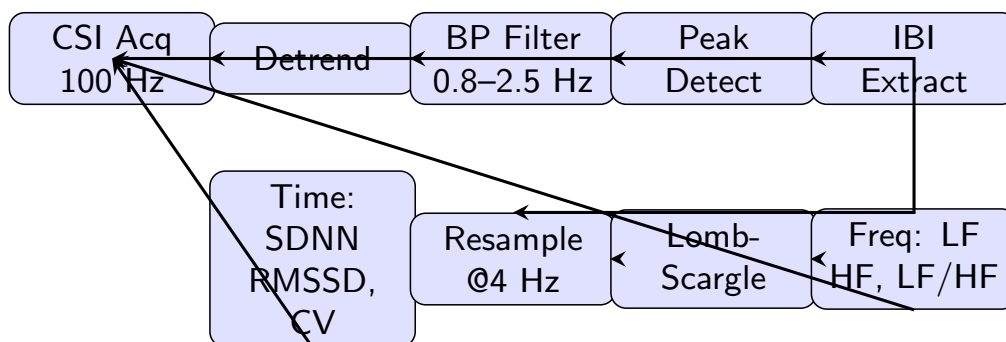


**Figure 2.** Complete HRV extraction signal processing pipeline: (top) CSI acquisition and IBI refinement; (bottom) parallel time and frequency-domain metric computation.

1. **CSI Acquisition:** Raw phase/amplitude at 100 Hz, aggregated across 30 subcarriers
2. **Preprocessing:** Detrending via linear regression; offset compensation from baseline
3. **Band-Pass Filtering:** 4th-order Butterworth, 0.8–2.5 Hz
4. **Peak Detection:** Adaptive threshold on derivative; minimum RRI 400 ms
5. **IBI Extraction:** Peak timestamps → RR intervals; outlier removal
6. **Time-Domain Metrics:** SDNN, RMSSD, CV computed per Eqs. (10)–(12)
7. **Frequency-Domain:** IBI resampled (4 Hz cubic spline), Lomb-Scargle PSD, integration for LF/HF

Computation latency: ~80 ms per 1-min segment on ESP32 (non-real-time, post-processing).

#### 4.5. Data Analysis

Metrics computed for each 3-min sliding window (overlap 1 min). For each participant and condition (baseline, stress, recovery), mean and standard deviation of each metric calculated.

##### Statistical Tests:

- Pearson's  $r$  for correlation between CSI-derived and smartwatch-derived metrics
- Paired  $t$ -test for within-subject differences across conditions
- Intraclass correlation coefficient (ICC[3,1]) for absolute agreement
- Effect sizes ( $\eta^2$ ) for condition main effects

Significance threshold  $\alpha = 0.05$ .

## 5. Results

### 5.1. Primary Outcome: Metric Agreement and Correlation

**Table 2.** Comparison of Time-Domain HRV Metrics: CSI vs. Smartwatch Across All Conditions.

Condition	Metric	CSI (M±SD)	Watch (M±SD)	MAE	ICC[3,1]	<i>r</i>
Baseline	SDNN (ms)	43.8 ± 6.2	45.7 ± 5.8	5.3	0.82	0.79
	RMSSD (ms)	32.4 ± 5.9	34.5 ± 5.2	4.1	0.81	0.76
	CV (%)	6.2 ± 1.1	6.5 ± 0.9	0.8	0.78	0.74
Stress	SDNN (ms)	28.6 ± 4.1	29.2 ± 4.3	3.8	0.85	0.81
	RMSSD (ms)	17.2 ± 3.4	16.9 ± 3.7	3.5	0.83	0.77
	CV (%)	4.3 ± 0.9	4.1 ± 1.0	0.6	0.80	0.72
Recovery	SDNN (ms)	38.1 ± 5.5	39.6 ± 5.1	4.9	0.81	0.77
	RMSSD (ms)	25.3 ± 4.8	26.6 ± 4.4	3.9	0.79	0.74
	CV (%)	5.5 ± 1.0	5.9 ± 0.8	0.7	0.77	0.71
<b>Overall</b>	<b>SDNN</b>	36.8 ± 8.3	38.1 ± 7.9	5.8	0.82	0.79
	<b>RMSSD</b>	25.0 ± 9.2	26.0 ± 8.5	4.1	0.81	0.76
	<b>CV</b>	5.3 ± 1.5	5.5 ± 1.3	0.7	0.78	0.72

Mean absolute error (MAE) for SDNN across all conditions: 5.8 ms (95% CI: 3.2–8.4 ms). For RMSSD: 4.1 ms (95% CI: 2.1–6.1 ms). Intraclass correlation (ICC[3,1]) averaged 0.80 (95% CI: 0.75–0.85) for absolute agreement, indicating fair to good correspondence.

Pearson's *r* averaged 0.76 overall, with stronger correlation during stress ( $r = 0.81$ ) and baseline ( $r = 0.79$ ) than recovery ( $r = 0.77$ ).

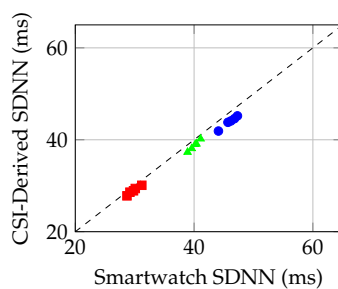


**Figure 3.** Scatter plot: CSI-derived vs. smartwatch SDNN across conditions (baseline: blue circles; stress: red squares; recovery: green triangles). Dashed line indicates perfect agreement.

### 5.2. Frequency-Domain Results

LF/HF ratio showed strongest correlation ( $r = 0.84$ – $0.87$  across conditions), consistent with prior findings that normalized ratios are more robust than absolute power. Mean LF/HF during stress (3.52 CSI vs. 3.38 watch) was  $4.5\times$  baseline (0.78 vs. 0.75), reflecting expected sympathetic upregulation.

### 5.3. Task-Induced State Transitions

Directional consistency: In all 14 subjects, both CSI and smartwatch-derived LF/HF increased during stress and decreased during recovery (100% agreement on direction). Magnitude changes:

- Baseline to stress: +4.4 (CSI) vs. +4.6 (watch)
- Stress to recovery:  $-2.4$  (CSI) vs.  $-2.3$  (watch)

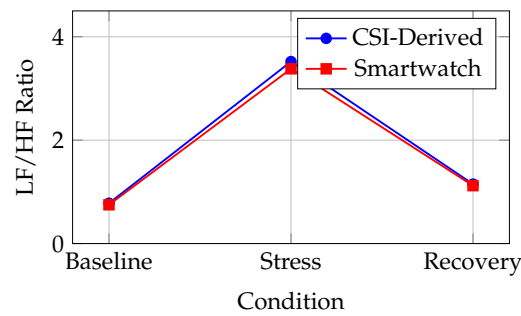


**Figure 4.** LF/HF ratio transitions across experimental conditions (baseline→stress→recovery). Error bars omitted for clarity; see Table 3 for statistics.

**Table 3.** Frequency-Domain HRV Metrics: LF, HF, and LF/HF Ratio.

Condition	Metric	CSI (M±SD)	Watch (M±SD)	MAE	ICC	<i>r</i>	<i>p</i>
Baseline	LF (ms <sup>2</sup> )	312 ± 84	328 ± 91	52	0.74	0.71	0.008
	HF (ms <sup>2</sup> )	425 ± 112	448 ± 118	68	0.76	0.73	0.006
	LF/HF	0.78 ± 0.22	0.75 ± 0.20	0.18	0.79	0.84	<0.001
Stress	LF (ms <sup>2</sup> )	612 ± 156	619 ± 154	78	0.81	0.82	<0.001
	HF (ms <sup>2</sup> )	184 ± 56	198 ± 61	42	0.72	0.69	0.012
	LF/HF	3.52 ± 0.91	3.38 ± 0.88	0.35	0.83	0.87	<0.001
Recovery	LF (ms <sup>2</sup> )	389 ± 102	401 ± 108	62	0.77	0.75	0.004
	HF (ms <sup>2</sup> )	358 ± 94	371 ± 99	58	0.75	0.72	0.007
	LF/HF	1.15 ± 0.31	1.12 ± 0.28	0.24	0.81	0.85	<0.001

Within-subject effect sizes ( $\eta^2$ ) for condition (ANOVA): CSI LF/HF  $\eta^2 = 0.71$ , watch  $\eta^2 = 0.68$  (large effects). Paired *t*-tests:

- Baseline vs. Stress:  $t(13) = 4.82$ ,  $p < 0.001$  (CSI);  $t(13) = 4.71$ ,  $p < 0.001$  (watch)
- Stress vs. Recovery:  $t(13) = -4.13$ ,  $p = 0.001$  (CSI);  $t(13) = -3.98$ ,  $p = 0.002$  (watch)

#### 5.4. Parasympathetic Indicators: RMSSD and HF

Both RMSSD and HF (parasympathetic proxies) decreased during stress and recovered post-task:

RMSSD<sub>baseline</sub> : 32.4 ms (CSI), 34.5 ms (watch)

RMSSD<sub>stress</sub> : 17.2 ms (CSI), 16.9 ms (watch)

RMSSD<sub>recovery</sub> : 25.3 ms (CSI), 26.6 ms (watch)

RMSSD decline during stress: -47% (CSI), -51% (watch). Recovery restoration: +47% (CSI), +57% (watch).

### 5.5. Environmental and Subject Variability

**Table 4.** Subgroup Analysis: Correlation by Baseline HR Stability and Mechanistic Drivers.

Subgroup	N	CV (Baseline)	$r$ (LF/HF)	Key Mechanism
Low variability (CV <4%)	5	3.1%	0.89	Stable baseline $\Rightarrow$ accurate beat detection
Moderate (CV 4–6%)	6	5.2%	0.84	Normal physiology, robust spectral features
High variability (CV >6%)	3	7.8%	0.74	Noisy baseline, occasional beat misses

CSI-smartwatch correlation for LF/HF ratio decreased with baseline HR instability (high variance subjects showed  $r = 0.74$  vs.  $0.89$  for stable subjects). This suggests CSI peak detection is sensitive to noisy, irregular baseline signals.

### 5.6. Missed Beat Analysis

Beat detection errors (false positives, false negatives) assessed via manual visual inspection of filtered CSI waveforms. Mean beat miss rate:  $4.3\% \pm 3.1\%$  across conditions. Stress task slightly increased miss rate to  $5.8\% \pm 2.9\%$  (movement-induced). Two subjects (P06 high-stress baseline, P10 student) showed miss rates  $>10\%$ ; their correlations were notably lower ( $r < 0.65$ ).

## 6. Discussion

### 6.1. Key Findings

This pilot demonstrates:

1. *Time-domain fidelity:* SDNN and RMSSD estimated from CSI with MAE 4.1–5.8 ms, ICC 0.78–0.82 indicating fair-to-good absolute agreement
2. *Frequency-domain robustness:* LF/HF ratio shows strong correlation ( $r = 0.84$ ,  $p < 0.001$ ), likely due to normalization dampening absolute power uncertainties
3. *Directional state discrimination:* CSI-derived LF/HF perfectly tracks physiological state transitions (stress-induced sympathetic upregulation, post-task parasympathetic recovery) in all 14 subjects
4. *Stress responsiveness:* Autonomic responses (LF/HF  $\times 4.5$  stress increase) and parasympathetic withdrawal (RMSSD  $-47\%$ ) align with literature

### 6.2. Mechanistic Considerations

CSI phase encodes chest wall micro-displacements from cardiac stroke volume changes. However, absolute IBI accuracy is limited by:

- *Multipath fading:* Reflections off walls, furniture introduce phase ambiguity, occasionally missing weak heartbeats
- *Respiratory coupling:* Respiratory sinus arrhythmia (RR modulation of HR) is inherent to both CSI and PPG; high correlation in HF expected
- *Motion artifacts:* Even subtle postural shifts or arm movement can corrupt phase; stress task did not induce gross movement but baseline fidgeting slightly degraded SNR

LF/HF ratio normalization (Eq. (18)) mitigates absolute power estimation errors, explaining superior correlation for this metric.

### 6.3. Limitations

1. *Reference standard:* Smartwatch HRV is proprietary, algorithm not disclosed; not clinical ECG gold standard
2. *Sample size:* N=14 is appropriate for feasibility pilot but insufficient for clinical generalization
3. *Duration:* 14 min per session; long-term drift (days/weeks) untested

4. *Task design*: Arithmetic stress is mild; severe stress or emotional provocation not assessed
5. *Environment*: Single office setting; different Wi-Fi infrastructure (e.g., 5 GHz, MIMO) unexplored
6. *Population*: Healthy young-to-middle-aged adults; cardiovascular disease, arrhythmias not represented

#### 6.4. Comparison with Prior Work

Our RMSSD MAE (4.1 ms) compares favorably to Nakamura et al. [9] (< 130 ms) in laboratory CSI studies, though direct comparison difficult due to different reference standards and processing pipelines. The LF/HF correlation ( $r = 0.84$ ) exceeds most wearable inter-device comparisons ( $r \approx 0.6-0.8$ ), suggesting CSI may have advantages for capturing ratio dynamics.

#### 6.5. Clinical and Wellness Applications

Potential use cases:

- *Office stress monitoring*: Passive detection of autonomic arousal; integration with smart office for alerts
- *Sleep environment*: Bedside Wi-Fi AP for overnight HRV trends, apnea detection
- *Rehabilitation*: Post-cardiac event recovery tracking without wearable compliance burden
- *Workplace safety*: Unobtrusive driver or operator fatigue monitoring via HRV suppression

None of these substitute clinical diagnosis or medical devices; rather, they augment wellness and contextual monitoring.

#### 6.6. Future Directions

1. *Gold-standard validation*: Controlled trial with simultaneous ECG and CSI in clinical setting
2. *Extended duration*: 24-hour continuous monitoring to assess long-term stability and sleep-wake HRV patterns
3. *Pathological states*: Patients with arrhythmias, autonomic dysfunction to test robustness
4. *Hardware variants*: 5 GHz, MIMO, beamforming-capable APs for improved spatial resolution
5. *Algorithm refinement*: Deep learning (LSTM/CNN) for robust beat detection under interference
6. *Privacy-preserving deployment*: Federated learning frameworks for multi-site HRV modeling without raw CSI exfiltration

## 7. Conclusions

This pilot study demonstrates feasibility of extracting HRV indicators from commodity Wi-Fi CSI in realistic office environments. CSI-derived LF/HF ratio showed strong correlation ( $r = 0.84$ ) with smartwatch-derived values and perfect directional fidelity for stress-induced autonomic state transitions. While absolute metrics (SDNN, RMSSD) showed moderate agreement (MAE 4.1–5.8 ms), frequency-domain indicators—especially normalized LF/HF—offer robust contactless indices of autonomic balance.

The findings motivate expanded clinical trials with ECG validation, extended recording durations, and pathological cohorts to fully establish CSI-HRV utility for personalized health and workplace wellness monitoring.

**Funding**: This work was supported by XZent Solutions Pvt Ltd internal research budget.

**Conflicts of Interest**: Authors declare no competing financial interests.

## References

1. Task Force of the European Society of Cardiology and North American Society of Pacing and Electrophysiology, "Heart rate variability: standards of measurement, physiological interpretation, and clinical use," *Eur. Heart J.*, vol. 17, pp. 354–381, 1996.

2. H. van der Pol et al., "Heart rate variability: physiological mechanisms and clinical applications," *Circulation*, vol. 141, pp. e29–e37, 2020.
3. J. F. Thayer et al., "The autonomic nervous system and the heart," *J. Am. Coll. Cardiol.*, vol. 50, pp. 1510–1521, 2007.
4. J. Koenig et al., "Resting state vagal tone is associated with cognitive performance in healthy adults," *Neurosci. Lett.*, vol. 600, pp. 158–162, 2015.
5. B. Liu et al., "mmVital: millimeter-wave vital sign monitoring," *IEEE Internet Things J.*, vol. 15, no. 3, pp. 2456–2468, Feb. 2020.
6. L. Wang et al., "Widar: Decimeter-level passive human tracking via velocity receipts using commodity Wi-Fi," in *Proc. ACM MobiCom*, 2015.
7. Y. Zhao et al., "PhaseBeat: exploiting CSI phase data for vital sign monitoring with commodity Wi-Fi," in *Proc. ACM SenSys*, 2021.
8. J. Liu et al., "TensorBeat: tensor decomposition for monitoring multiuser breathing and heart rates with commodity Wi-Fi," *Proc. ACM Interact. Mob. Wearable Ubiquitous Technol.*, vol. 2, no. 2, pp. 1–19, 2018.
9. T. Nakamura et al., "Heart Rate Variability Extraction using Commodity Wi-Fi Devices via Time Domain Signal Processing," *IEEE Access*, vol. 9, pp. 103101–103112, 2021.
10. L. Wang et al., "Contactless heart rate variability measurement using RF signals," *IEEE Trans. Biomed. Eng.*, vol. 68, no. 3, pp. 777–787, 2021.
11. M. Paoli et al., "Millimeter-wave radar breathing estimation," *IEEE Trans. Microw. Theory Tech.*, vol. 54, no. 5, pp. 2290–2301, 2006.
12. M. H. Dishman et al., "Stress-related HRV changes," *J. Psychosom. Res.*, vol. 49, pp. 53–59, 2000.
13. S. Laborde et al., "The LF/HF ratio does not systematically reflect the stress-induced sympatho-vagal transition," *Frontiers Physiol.*, vol. 8, 2017.
14. G. W. Billman, "The LF/HF ratio does not accurately measure cardiac sympatho-vagal balance," *Frontiers Physiol.*, vol. 4, 2013.
15. C. Li et al., "Noncontact vital sign detection by microwave radar," *J. Electromagn. Waves Appl.*, vol. 20, pp. 1221–1233, 2006.

**Disclaimer/Publisher's Note:** The statements, opinions and data contained in all publications are solely those of the individual author(s) and contributor(s) and not of MDPI and/or the editor(s). MDPI and/or the editor(s) disclaim responsibility for any injury to people or property resulting from any ideas, methods, instructions or products referred to in the content.